OPENFOAM 3D Modeling of Melt Spinning Process in Non-Planar Geometry

A. Maroni[1], M. Pagnola[2,a], J. Moya[1], M. Malmoria[2]

[a]mpagnola@fi.uba.ar
[1]Grupo Interdisciplinario en Materiales, INTECIN UBA-CONICET, IESIING
Universidad Católica de Salta
Argentina
[2]University of Buenos Aires,
National Council of Scientific and Technical Research,
Institute of Technology and Engineering Sciences 'Hilario Fernández Long' (INTECIN),
Buenos Aires, Argentina

Abstract

Melt spinning is an industrial process used for the production of metallic glasses. It is a rapid solidification process whereby a liquid metal is ejected at high pressure and temperature via a nozzle onto a rotating copper wheel by solidifying in the form of a thin ribbon. In this work, we perform a 3D simulation model to reproduce the melt spinning process to get amorphous magnetic material, starting from an alloy with chemical composition $Fe_{75}Si_{10}B_{15}$(% at.). A ***CFD*** model in the OpenFoam® open source code is proposed and applied, which is based on the Finite Volume Method (***FVM***) and Volume of Fluid Method (***VOF***). The entire process without solidification is analyzed simply as a preliminary study of the ejection conditions during the melt, in order to avoid posterior turbulence in the film that would cause irregularities in subsequent stages of solidification. This preliminary analysis aims to study the generation of a regular film of molten material on a rotating cylindrical geometry. In the ***FVM*** method the coupled incompressible laminar momentum and continuity equations are solved at each time step on every mesh cell, while in the ***VOF*** scheme the fluid properties are weighed average of those of air and molten metal. The complete geometry is discretized in a block-structured mesh of pure hexahedra. The profile and dimensions of the resulting meniscus and ribbon during the transient are in good agreement with our previous numerical results.

Key Words: Melt Spinning, Solidification, Magnetic Materials, OpenFOAM®, CFD, Volume of Fluid, Numerical Methods for Multiphase Flow

1 Introduction

Metallic alloys and materials of amorphous and nanocrystalline structure have found widespread applications in industry and science. Therefore, the study and further improvement of industrial processes involved in their manufacturing is an active area of engineering research and development, attracting interest and effort from many scientific disciplines [1]. One of the most popular and promising of those production methods, the Chill Block Melt Spinning (CBMS), consists basically in an ultra-fast, almost instantaneous, solidification of molten material induced upon contact with a rotating cold surface. This way, very thin ribbons of relatively continuous width and thickness can be easily produced of desired lengths, possessing uniform material structure ranging from amorphous to nanocrystalline, depending on some variables process such as chemical composition of the alloy, velocities, temperatures, pressures of the process, etc. In the literature [2],

[3], [4], [5], and [6], there are some works where it is intended to model these parameters either mathematically or numerically. In this work we present our first results using the ***OpenFOAM™*** software to simulate, in ***3D***, the process prior to solidification and formation of the ribbon, taking into account pressures and velocities of the process and the viscosity of a $\boldsymbol{Fe_{75}Si_{10}B_{15}}$ alloy.

2 Outline of the CBMS Process

In spite of its apparent simplicity, CBMS involves a large number of process variables, some much harder to define and control than others, intertwined in complex chemical and mechanical interactions. Chemical variables, like alloy composition and controlled atmosphere, are usually fixed at the very beginning, whereas a small set of geometric variables, like nozzle-wheel gap and wheel width, are standardized according to the use of the ribbon as a final product.

3 Governing Equations and Numerical Method

The incompressible, viscous, time-dependent Navier-Stokes and continuity equations govern the mechanics of the fluid flow in a simple, connected domain Ω:

$$\begin{aligned} \partial_t \mathbf{u} + \mathbf{u} \cdot \nabla \mathbf{u} &= -\nabla p + \nu \nabla^2 \mathbf{u}, \qquad && x \in \Omega, \\ \nabla \cdot \mathbf{u} &= 0, && x \in \Omega. \end{aligned}$$

Let us first partition our fluid flow domain into non-overlapping polyhedral control volume cells, so that, by integrating the first of equations (1) over cell k, and applying the divergence theorem, we arrive at:

$$\mathbf{V}_k \frac{\partial u_i}{\partial t} + \oint_k u_i \mathbf{u} \cdot d\mathbf{A} = \oint_k \nu \overrightarrow{\nabla u_i} \cdot d\mathbf{A} - \oint_k p \hat{\boldsymbol{\imath}}_i \cdot d\mathbf{A},$$

where V_k is the volume of cell k, $\widehat{\imath}_i$ is the i-the orthonormal unit vector in the spatial basis, and the surface integrations are performed over the entire control volume boundary. Carrying out low order surface integrations, we obtain a discrete set of algebraic equations for each cell k:

$$\mathbf{V}_k \frac{\partial u_i}{\partial t} = \sum_{\text{Faces of } k} \left\{ \nu \sum \frac{\partial u_i}{\partial x_j} A_j - p A_i - u_i \sum u_j A_j \right\}_{\text{face}},$$

in which face pressure and velocity, as used in left-hand-side calculations, are taken as the face averages. Simultaneously, pressure must be calculated by solving the Poisson equation that results from the system of equations (1):

[Warning: Image ignored]

Where $\mathrm{L} = \nabla \mathrm{u}$ is the velocity gradient tensor. Methods to solve equations (3) and (4) include SIMPLE, SIMPLER, SIMPLEC, PISO, etc. Briefly speaking, the **VOF** method solves the above system of equations for a fluid whose physical properties are weighted averages of those of the two fluids present in a cell. The weight used, denoted γ, is such that, in any cell, the actual mass density is

$$\rho = \gamma \rho_{fluid1} + (1 - \gamma)\, \rho_{fluid2},$$

so that γ can also be called void fraction of fluid 1. A scalar transport equation is used to model the void fraction. Also, an extra term is added to ∇p to account for the surface tension force at the free surfaces, which is the interface between both fluids.

4 Domain Geometry and Grid Generation

The entire simulation domain, consisting of crucible, nozzle, and the atmospheric body around the gap, between nozzle and wheel, is 3D-modelled with dimensions as shown in ***Figure 1.***

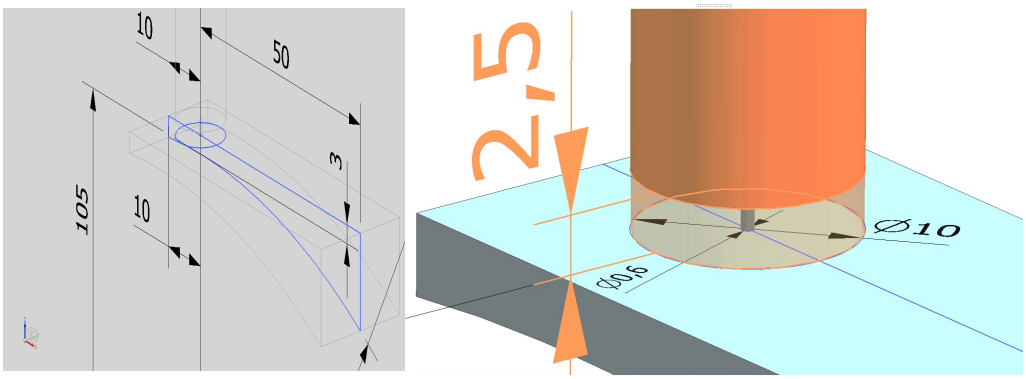

Figure 1. Dimensions of the atmospheric sub-domain extrusion (left) and of the gap and crucible (right).

A spatial discretization is carried out by dividing the domain into simply connected structured blocks, as shown in ***Figure2.a.*** Boundary layer clustering is applied on the wheel wall as well as along the ribbon and puddle, as depicted in ***Figure 2.b***, in which only the nozzle mesh is shown, along with the grid in the nozzle and around the puddle.

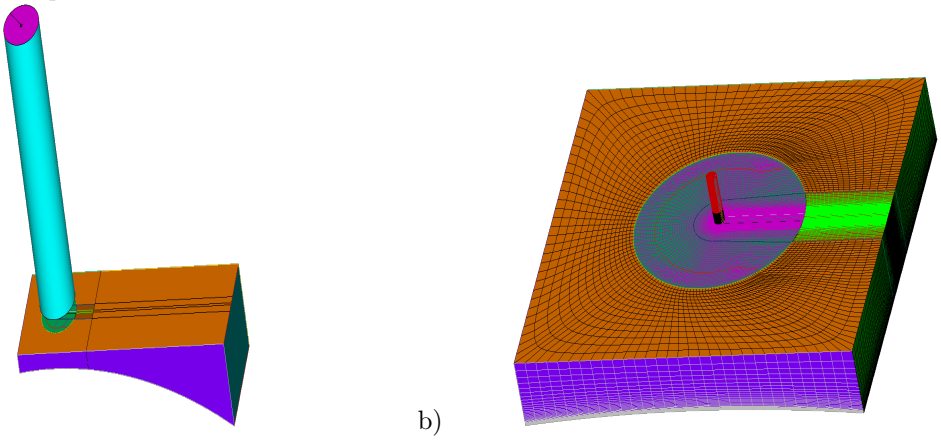

a) b)

Figure 2. a) Block partitioning for discretization. b) Detail of meshing in area around the gap and nozzle.

The total number of resulting finite volume cells was 556k Hexas, mostly clustered in the gap area shown in ***Figure 2.b.***

5 Fluid Properties and Flow Parameters

Phase 1 is set as air at 20 ℃, with $\rho = 1.225 kg/m^3$ and $\mu = 1.7894 \bullet 10^{-5} Ns/m^2$, whereas phase 2 is a molten $Fe_{75}Si_{10}B_{15}$ alloy with $\rho = 7400 kg/m^3$ and $\mu = 5.51 \bullet 10^{-2} Ns/m^2$. The surface tension force has been modeled using the "Continuum Surface Stress" scheme, with $\sigma = 0.367 N/m$. The working atmospheric pressure is 1 atm and the wheel tangential velocity is 40 m/s. The molten alloy flow rate at the nozzle was regulated partly by setting a crucible metal load height of almost 50 mm, and fine-tuned with a flow rate at the crucible top face.

6 Main Results

Time integration was performed with a first order implicit Euler scheme which allowed for greater ***CFL*** flexibility than the explicit method. Therefore, a fixed time step was used that was small enough to have the molten material cross the gap in at least 10 time steps. As expected, the molten metal forms a poodle on hitting the cold copper wheel, as shown in ***Figure 3***, then winds down into a ribbon, which, after a few centimeters, settles at a uniform width of $1.12 \bullet 10^{-3} m$ and a thickness of $37.05 \bullet 10^{-6} m$, as depicted in ***Figure 4.a*** and ***4.b.*** Boundary layer contours were also added in ***Figures 3.a*** and ***4.b***. These values are in close agreement with *Pagnola et al.*[7]

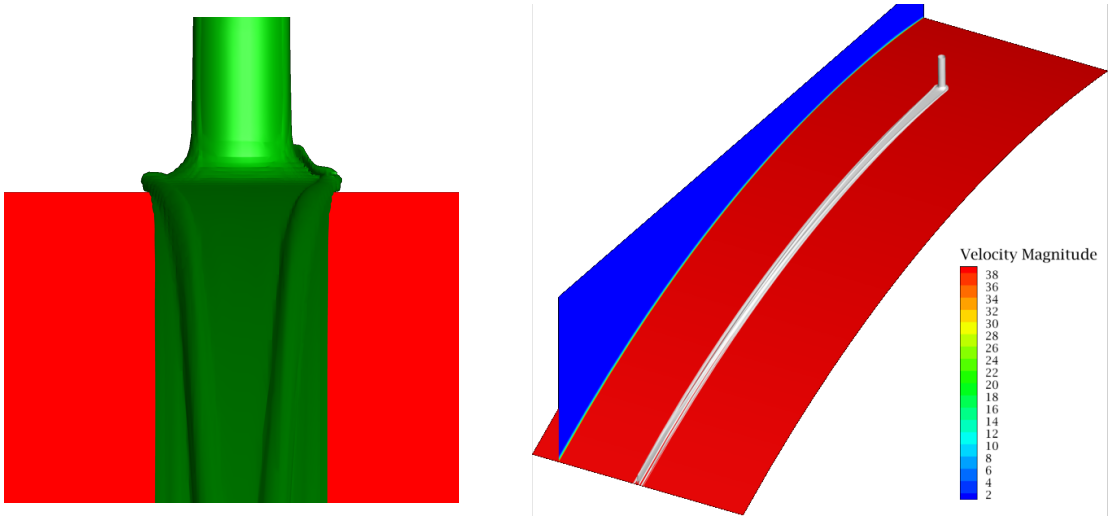

Figure 3. Ribbon at last time step, a) isometric view, b) and front view.

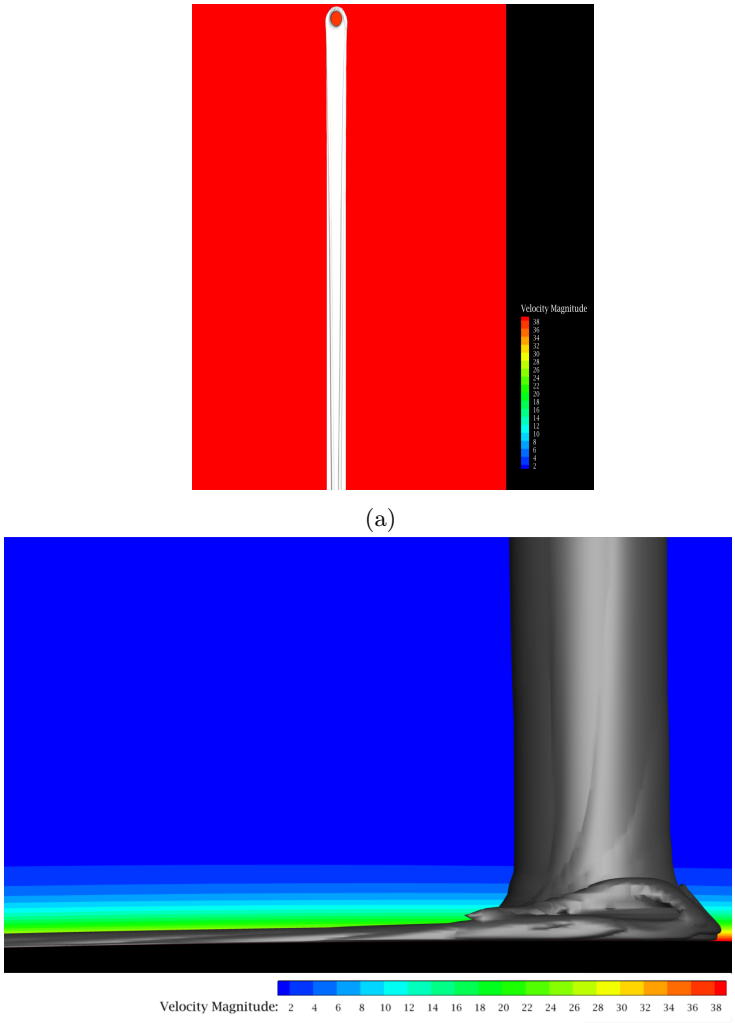

(a)

(b)

Figure 4. Ribbon at last time step, a) upper view, and b) side view.

7 Conclusions

Full ***3D CFD*** simulations of ***CBMS*** casting process have been performed in ***OpenFOAM™*** which continue our previous work [8], and, whereas based on the same model equations and displaying very good agreement with their results, add the obvious advantages of producing fully ***3D*** meniscus along with ribbon texture and features not seen in their work. This encourages us to continue our work by incorporating extra multi-physics modeling, i.e., heat transfer and solidification in future researches that complete the progress made [7,8].

References

[1] V.P. Sharma, U. Sharma, M. Chattopadhyay, V.N. Shukla, Advance Applications of Nanomaterials: A Review, Materials Today: Proceedings, Elsevier, Volume 5, Issue 2, Part 1, 2018, Pages 6376-6380.doi: doi.org/10.1016/j.matpr.2017.12.248.

[2] H.H. Liebermann, The dependence of the Geometry of glassy alloy ribbons on the chill block melt-spinning process parameters, Mater. Sci. Eng. 43 (1980) 203–210. doi:10.1016/0025-5416(80)90103-2.

[3] Y.K. Li, Y. Yang, Y.M. Song, F.R. Zhang, Numerical Simulation of Flow and Heat Transfer for Cooling Roller in Amorphous Spinning Process, Adv. Mater. Res. 1142 (2017) 276–281. doi:10.4028/www.scientific.net/AMR.1142.276.

[4] G.-X. Wang, E.F. Matthys, Modelling of rapid solidification by melt spinning: effect of heat transfer in the cooling substrate, Mater. Sci. Eng. A. 136 (1991) 85–97. doi:10.1016/0921-5093(91)90444-R.

[5] V.I. Tkatch, S.N. Denisenko, B.I. Selyakov, Computer simulation of Fe80B20 alloy solidification in the melt spinning process, Acta Metall. Mater. 43 (1995) 2485–2491. doi:10.1016/0956-7151(94)00413-7.

[6] V.I. Tkatch, A.I. Limanovskii, S.N. Denisenko, S.G. Rassolov, The effect of the melt-spinning processing parameters on the rate of cooling, Mater. Sci. Eng. A. 323 (2002) 91–96. doi:10.1016/S0921-5093(01)01346-6.

[7] M.R. Pagnola, M. Barone, M. Malmoria, H. Sirkin, Influence of z /w relation in Chill Block Melt Spinning (CBMS) process and analysis of thickness in ribbons, Multidiscip. Model. Mater. Struct. 11 (2015) 23–31. doi:10.1108/MMMS-02-2014-0008.

[8] M. Pagnola, M. Malmoria, M. Barone, Biot number behaviour in the Chill Block Melt Spinning (CBMS) process, Appl. Therm. Eng. 103 (2016) 807–811. doi:10.1016/j.applthermaleng.2016.04.077.